AIP Applied Physics Letters

Laser energy tuning of carrier effective mass and thermopower in epitaxial oxide thin films

A. I. Abutaha, S. R. Sarath Kumar, and H. N. Alshareef

Citation: Applied Physics Letters **100**, 162106 (2012); doi: 10.1063/1.4704183
View online: http://dx.doi.org/10.1063/1.4704183
View Table of Contents: http://scitation.aip.org/content/aip/journal/apl/100/16?ver=pdfcov
Published by the AIP Publishing

Laser energy tuning of carrier effective mass and thermopower in epitaxial oxide thin films

A. I. Abutaha, S. R. Sarath Kumar, and H. N. Alshareef[a)]
Materials Science and Engineering, King Abdullah University of Science and Technology (KAUST), Thuwal 23955-6900, Saudi Arabia

(Received 13 January 2012; accepted 27 March 2012; published online 18 April 2012)

The effect of the laser fluence on high temperature thermoelectric properties of the La doped $SrTiO_3$ (SLTO) thin films epitaxially grown on $LaAlO_3$ ⟨100⟩ substrates by pulsed laser deposition is clarified. It is shown that oxygen vacancies that influence the effective mass of carriers in SLTO films can be tuned by varying the laser energy. The highest power factor of 0.433 W K^{-1} m^{-1} has been achieved at 636 K for a film deposited using the highest laser fluence of 7 J cm^{-2} $pulse^{-1}$.
 [http://dx.doi.org/10.1063/1.4704183]

$SrTiO_3$ (STO) is a promising n-type oxide suitable for high-temperature thermoelectric applications.[1–5] The melting point[6] of STO is 2353 K making it applicable at high temperatures, unlike the heavy metal based materials such as Bi_2Te_3 and PbTe, which are not stable at temperatures in excess of 1000 K. Moreover, the constituents of STO are all naturally abundant compared to other conventional thermoelectric materials. The electrical conductivity of STO can be easily varied from insulating to metallic by the substitutional doping with La^{3+} or Nb^{5+} and also by creating oxygen vacancies.[2,4] In spite of all the attractive features, the figure of merit ZT ($ZT = \sigma S^2 T/\lambda$, where σ is the electrical conductivity, S is the Seebeck coefficient, T is the absolute temperature, and λ is the thermal conductivity) of STO is smaller than that of the heavy metal based materials, since STO has a relatively high thermal conductivity (3–10 W m^{-1} K^{-1}).[1] Recently, several research groups reported relatively high ZT for STO with La doping (0.21 at 750 K)[7] and Dy and La doping (0.36 at 1045 K).[8] Considerable improvement in ZT is required to make STO, a practical thermoelectric material and one way to do so is to reduce the thermal conductivity by nano structuring or doping with elements that enhance mass-fluctuation scattering. On the other hand, enhancing the electron transport properties is often limited by the trade-off relationship between σ and S in terms of electrical mobility (μ). For example, with increasing μ, σ increases while S decreases. Optimizing the growth conditions of the thin films is hence important to achieve the best power factor. The oxygen content and hence the carrier concentration (n) plays a vital role in detemining the physical properties of the films. The usual sources of oxygen in oxide films grown by pulsed laser deposition (PLD) are the background gas and the substrate.[9,10] It has been reported that Hall mobility of carriers at room temperature decreases as oxygen pressure increases, and hence oxygen partial pressure strongly affect the electrical transport properties of the PLD grown $Sr_{0.98}La_{0.02}TiO_{3-\delta}$ (SLTO) thin films.[9] Another approach to improve the power factor is by forming high density two-dimensional electron gas confined in a very thin layer of STO to produce a large value of $|S|$ (850 μV K^{-1}) without reducing electrical conductivity.[1] The effective mass (m^*) of electrons is an important physical quantity that the electrical properties depend on. By changing the dopant concentration, m^* can be varied. In STO single crystals, m* has been reported to vary in the range 6–6.6 m_0 and 1.1–1.6 m_0 for La (Refs. 3 and 4) and in the range 7.3–7.7m_0 for Nb (Ref. 4) dopants.

In this work, we report the role of laser fluence in determining the oxygen content in STO based thermoelectric thin films. X-ray diffraction (XRD) and atomic force microscopy (AFM) have been used to characterize the thin films. The temperature dependence of the electrical conductivity and Seebeck coefficient has been measured for three different laser fluences. The electrical transport properties at 300 K have been determined by using a physical property measurement system (PPMS). The observed results are explained based on the dependence of effective mass on the oxygen content of the films.

SLTO films were deposited by PLD (Neocera, Beltsville, MD) using a KrF excimer laser ($\lambda = 248$ nm, pulse duration ~20 ns, and repetition rate = 10 Hz). Films were deposited by ablation of a 4 N purity SLTO target (Testbourne Ltd., England) at three different laser fluences (7, 6, and 5 J cm^{-2} $pulse^{-1}$) and are denoted as films I, II, and III, respectively. The target was held on a rotating carousel to ensure an uniform ablation from the target surface. In order to create sufficient oxygen vacancies, 20 mTorr of Ar was introduced as a reducing gas. The gas flow was regulated by a mass flow controller. Films were deposited on (100) oriented $LaAlO_3$ (LAO) substrates (MTI corporation, USA) of dimensions $10 \times 10 \times 0.5$ mm^3 with $a_{LAO} = 3.82$ Å, held at a temperature of 875 °C. The thickness of the films is around 500 nm as measured by a spectroscopic ellipsometer. The phase purity of the thin films was determined from the analysis of θ–2θ (Bragg-Brentano) and Φ (phi) scans using an x-ray diffractometer (D8 Bruker, AXS System, Germany). Φ scan was done for an asymmetric (110) diffraction of the SLTO thin film on LAO substrate. When ψ, the tilt angle of the surface normal of the film, was 45° and 2θ was fixed at 32.42°, Φ scan result was obtained by rotating the film (0°–360°) around the surface normal. The electrical conductivity and the Seebeck coefficient were measured from

a)Author to whom correspondence should be addressed. Electronic mail: husam.alshareef@kaust.edu.sa.

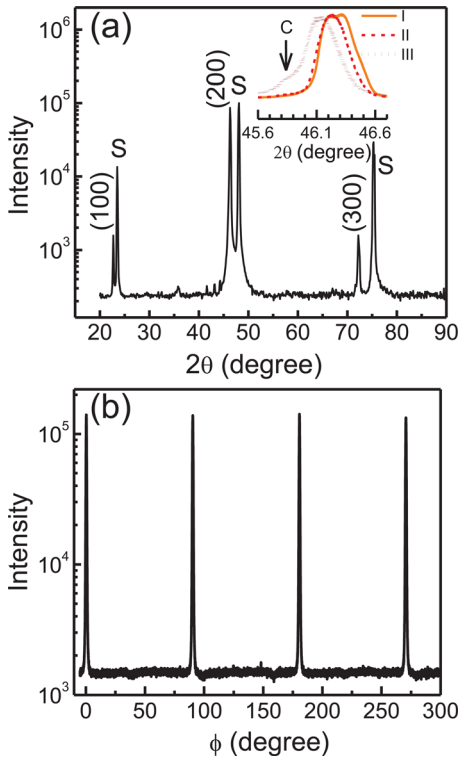

FIG. 1. θ-2θ XRD pattern (a) for SLTO thin films grown by different laser fluences on LAO substrate. The inset shows the fine scan for (200) reflection revealing the lattice expansion with decrease in laser fluence. Φ scan (b) for film II.

300–1000 K by using, respectively, the linear four-probe and the differential methods, under Ar/H_2 (4% H_2 and 96% Ar) ambient using a commercial setup (RZ2001i, Ozawa Science Co Ltd., Nagoya, Japan). Room temperature Hall effect was measured by using the PPMS (Quantum Design, Inc., USA). The surface morphology of the films was obtained by using AFM (Agilent, 5400, USA).

Figure 1(a) shows θ-2θ XRD patterns for the films. The diffraction peaks of the (100) planes from LAO (marked "S") and SLTO can be seen and reflections from other crystalline orientations are of negligible intensity, indicating a preferential epitaxial growth of the films on the substrate. Figure 1(b) shows the Φ scan for SLTO on LAO wherein four peaks with almost equal intensity spaced by 90° can be observed. The full width at half maximum (FWHM) of the peaks is 0.69°, indicating a low mosaic spread and a high quality of the epitaxial thin film growth. Fine scans in the θ-2θ geometry were done for (200) reflection from SLTO (inset to Fig. 1(a)) to detect any change in lattice constant with laser fluence in the films. The observed lattice constants of the films are presented in Table I. All films possess a higher lattice constant compared to stoichiometric STO (3.905 Å). The ionic radius of La^{3+} (1.5 Å) with co-ordination number 12 is smaller than that of Sr^{2+} (1.58 Å), which it substitutes. Hence, a decrease in lattice constant should be expected in SLTO films and hence the observed increase in lattice constant indicates the presence of oxygen vacancies in the films. In STO, oxygen binds the cations together in SrO and TiO_2 planes and hence for films with oxygen vacancies, the cation-cation overlap decreases, leading to an increase in lattice constant.[2,11] The systematic shift in (200) peak position indicates that the unit cell parameters of the films vary with laser fluence. The decrease in lattice constant with increase in laser fluence can be explained in terms of a decrease in oxygen vacancy concentration in the films. As the laser fluence increases, the oxygen content in the film increases. The plasma plume generated from the surface of the SLTO target has different ionic elements and clusters. The velocity of the plume species depends on different factors such as the mass, electrical charge of the species, laser fluence of the ablating laser, and partial pressure of the background gas.[12] Oxygen ions have the lowest mass compared to other species of the plume and possess a low magnitude (−2) of the electrical charge and hence have the highest velocities. Evidently oxygen ions reach the substrate first. At high laser fluence, more oxygen ions are bombarded towards the substrate where the nucleation takes place,[12] enabling growth of films with lower oxygen vacancy concentration. From the FWHM of the (200) peaks of the films I, II, and III, an average crystallite size of 55 nm was calculated by applying Scherrer's equation after taking into account the instrument broadening. For film III, the fine scan reveals a broader shoulder (denoted by "C"), which is indicative of a small cation non-stoichiometry.[13] However, from the shift of the (200) peak position, it is clear that oxygen vacancy concentration is highest in this film and hence the cation non-stoichiometry will have negligible influence in the transport properties of the films. On the contrary, if one assumes that the oxygen concentration in the films are the same, the deficiency of La, that can also explain the observed shift in the peak position, should lead to a marked reduction in carrier concentration in the n-type SLTO films, since each La ion contributes an electron to the conduction band and the deficiency of La may be treated as hole doping. However, as shown in Table I, the carrier concentrations of the films I, II, and III are, respectively, 3.635, 8.312, and 11.27 ($\times 10^{20}$ cm^{-3}) implying that the film with largest shift in the (200) peak has the highest carrier concentration and hence La deficiency can be ruled out. Moreover, if contribution from oxygen vacancies is ignored, using a simple

TABLE I. Measured and calculated transport properties of SLTO thin films at 300 K. m^*/m_0 is the effective mass of the carriers with respect to the rest mass of electron (m_0).

Sample No.	Lattice constant (Å)	Electrical conductivity (S cm^{-1})	Carrier concentration ($\times 10^{20}$ cm^{-3})	Hall mobility (cm^2 V^{-1} s^{-1})	Effective mass m^*/m_0	Seebeck coefficient, |S| (μV K^{-1})	Power factor (W K^{-1} m^{-1})
I	3.918	212	3.635	3.64	1.88	217	0.30
II	3.924	140	8.312	1.05	2.93	222	0.21
III	3.932	81	11.27	0.45	3.86	257	0.16

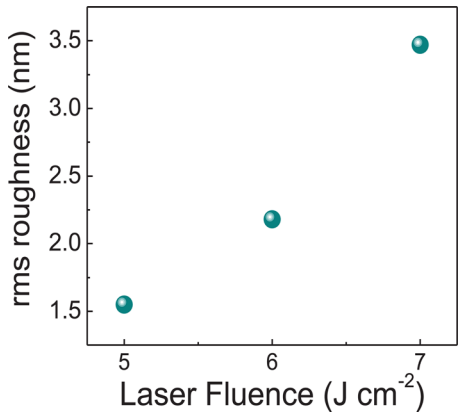

FIG. 2. Root mean square surface roughness of the films as a function of laser fluence.

calculation using the unit cell volume and assuming that all La atoms are ionized, with each La ion contributing an electron to the conduction band, it can be shown that approximately 2.1, 4.9, and 6.7 at. % of La is required to account for the observed carrier concentrations in films I, II, and III, respectively. Such large variations in La concentration are not probable, since the concentration of La in the target is only 2 at. %. Also, such an increase in La content should result in a decrease in lattice constant whereas the observed trend is the opposite. It must be noted that the observed carrier concentrations can be easily accounted for if we assume $Sr_{0.98}La_{0.02}TiO_{3-\delta}$ with $\delta = 0.0008$, 0.015, and 0.024, respectively, for films I, II, and III. These values of δ can be easily achieved in the PLD growth in 20 mTorr of Ar.

Figure 2 shows the dependence of rms roughness on the laser energy, the roughness generally increases with increasing the laser energy.[14] Films I, II, and III have rms roughness 3.47 nm, 2.18 nm, and 1.55 nm, respectively. Clearly, as the laser fluence increases, large ionic clusters will be ablated from the target. These bombarded constituents will not decompose completely before they arrive at the substrate surface because of their high velocity. At the same time, many incident atoms and ions will be re-sputtered from the substrate, which makes the surface rough during the nucleation process. The measured roughness values are approximately the same, and hence the difference in electron scattering in the films by surface roughness will be minimal.

The temperature dependence of electrical conductivity is plotted in Fig. 3. All the films behave as degenerate semiconductors in the temperature range of 300–1000 K. The contribution of the LAO substrate to electrical conductivity of SLTO is negligible because it is electrically insulating. At any temperature, film I has the highest electrical conductivity due to lowest effective mass of electrons as compared to the other films. In other words, the effective mass increases with lattice constant and carrier concentration.[3] This is an obvious indication of the dependence of effective mass of the electrons on laser fluence. In SLTO films, every La^{3+} ion that substitutes for Sr^{2+} ion contributes an electron each to the conduction band, provided all the dopant atoms are ionized. Similarly, each doubly ionized oxygen vacancy contributes two electrons to conduction. Hence carrier concentration of SLTO increases. Table I shows the electrical transport properties at 300 K of the SLTO thin films grown with different laser fluences. The Hall mobility was estimated by using the equation $\sigma = ne\mu$.[15] From Table I, it is evident that film III with the highest concentration of oxygen vacancies has the highest carrier concentration. However, since oxygen vacancies act as point scatterers, the mobility of film III is adversely affected, leading to a reduction in electrical conductivity.

The temperature dependence of Seebeck coefficient and power factor ($PF = S^2\sigma T$) are shown in Figs. 4(a) and 4(b), respectively. All films have negative Seebeck coefficient indicating n-type conduction as a consequence on La and oxygen vacancies doping of STO. The effective masses of the electrons in the films were estimated from the Seebeck coefficient around the room temperature, using the following equation:[15,16]

$$S = \frac{8\pi^{8/3}k_B^2 m^*}{3^{5/3}eh^2n^{2/3}}(r+1)T,$$

where $k_B, m^*, h, n, r,$ and T are the Boltzmann's Constant, effective mass, Planck's constant, carrier concentration, carrier scattering parameter of the relaxation time, and absolute temperature, respectively. From the slope of the S–T curve at

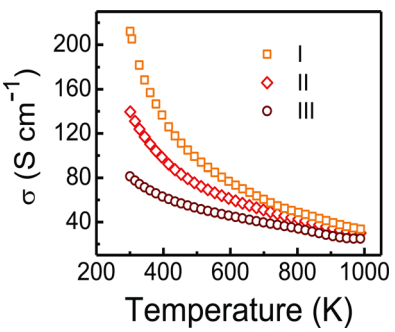

FIG. 3. Electrical conductivity for the films grown with different laser fluences.

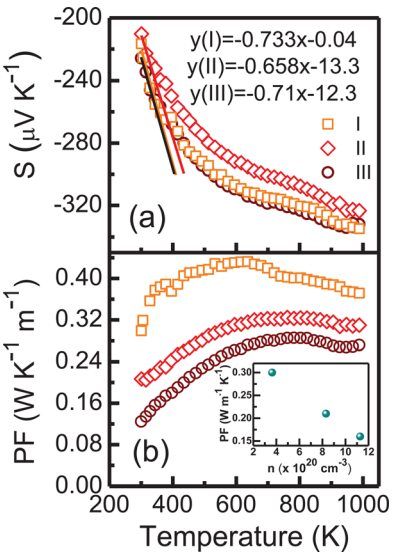

FIG. 4. The temperature dependence of (a) Seebeck coefficient and (b) power factor for SLTO thin films grown by different laser fluences. The inset to (b) shows the power factor dependence on carrier concentration.

temperatures below the Debye temperature[17] of the $SrTiO_3$ ($\theta_D = 513$ K), the effective mass of the films can be extracted by assuming $r = 2$ (ionized impurity scattering). This assumption is valid near room temperature, since scattering by acoustic phonons can be neglected below θ_D. Above θ_D, the slope of the *S–T* curve changes, and this is attributed to changes in electron scattering mechanism. Electrons are scattered predominantly by acoustic phonons above θ_D. The temperature dependence of the derived power factor (W K^{-1} m^{-1}) is plotted in Fig. 4(b). Film I exhibits the best power factor within the whole temperature range (0.433 W K^{-1} m^{-1}) at 636 K, which compares well with those reported for 0% La doped STO (0.23 W K^{-1} m^{-1}), 5% La doped STO (0.93 W K^{-1} m^{-1}) (Ref. 2) at 375 K, and 10% Nb doped STO (0.6 W K^{-1} m^{-1}) (Ref. 5) at 1000 K. Inset to Fig. 4(b) shows the variation of power factor with carrier concentration for the SLTO films. It is seen that the film with the lowest carrier concentration has the highest power factor. Recently, it has been reported that oxygen vacancies in STO lead to a decrease in the thermal conductivity.[18] Hence, by tuning the oxygen vacancies, large increase in ZT may be achieved, since oxygen vacancies, if controlled, can increase the electronic contribution with a simultaneous reduction in thermal conductivity.

In summary, we showed the effect of laser energy on the thermoelectric response of SLTO thin films in the temperature range 300–1000 K. In PLD process, the coating of laser window by the ablated species, with sequential depositions is a source of uncertainty of actual laser energy falling on the target. For wide band-gap materials such as SLTO, this coating effect results in a significant drop of laser energy falling on the target, but often goes undetected to the bare eye. As demonstrated in this work, the variation in laser energy affects the dynamics of film growth. As the laser fluence increases, the oxygen concentration decreases, resulting in an enhancement in carrier concentration and electron effective mass, which determines the thermoelectric power factor of the films. The best power factor obtained in this work is 0.433 W K^{-1} m^{-1} at 636 K for 7 J cm^{-2} $pulse^{-1}$, which agrees well with those reported in literature.

[1]H. Ohta, S. Kim, Y. Mune, T. Mizoguchi, K. Nomura, S. Ohta, T. Nomura, Y. Nakanishi, Y. Ikuhara, M. Hirano, H. Hosono, and K. Koumoto, Nature Mater. **6**(2), 129 (2007).
[2]J. Ravichandran, W. Siemons, D. W. Oh, J. T. Kardel, A. Chari, H. Heijmerikx, M. L. Scullin, A. Majumdar, R. Ramesh, and D. G. Cahill, Phys. Rev. B **82**(16), 165126 (2010).
[3]T. Okuda, K. Nakanishi, S. Miyasaka, and Y. Tokura, Phys. Rev. B **63**(11), 113104 (2001).
[4]S. Ohta, T. Nomura, H. Ohta, and K. Koumoto, J. Appl. Phys. **97**(3), 034106 (2005).
[5]S. Ohta, T. Nomura, H. Ohta, M. Hirano, H. Hosono, and K. Koumoto, Appl. Phys. Lett. **87**(9), 092108 (2005).
[6]H. Ohta, Mater. Today **10**(10), 44 (2007).
[7]J. Liu, C. L. Wang, W. B. Su, H. C. Wang, P. Zheng, J. C. Li, J. L. Zhang, and L. M. Mei, Appl. Phys. Lett. **95**(16), 162110 (2009).
[8]H. C. Wang, C. L. Wang, W. B. Su, J. Liu, Y. Zhao, H. Peng, J. L. Zhang, M. L. Zhao, J. C. Li, N. Yin, and L. M. Mei, Mater. Res. Bull. **45**(7), 809 (2010).
[9]S. Liang, D. J. Wang, J. R. Sun, and B. G. Shen, Solid State Commun. **148**(9–10), 386 (2008).
[10]C. W. Schneider, M. Esposito, I. Marozau, K. Conder, M. Doebeli, Y. Hu, M. Mallepell, A. Wokaun, and T. Lippert, Appl. Phys. Lett. **97**(19), 192107 (2010).
[11]W. Wunderlich, H. Ohta, and K. Koumoto, Phys. B: Condens. Matter **404**(16), 2202 (2009).
[12]C. W. Schneider and T. Lippert, *Laser Processing of Materials,* Springer Series in Materials Science, edited by Peter Schaaf (Springer, Berlin, 2010), Vol. 139, p. 89.
[13]B. Jalan, P. Moetakef, and S. Stemmer, Appl. Phys. Lett. **95**(3), 032906 (2009).
[14]M. Liu, B. Man, X. Lin, and X. Li, J. Cryst. Growth **311**(4), 1087 (2009).
[15]R. A. Smith, *Semiconductors* (Cambridge University Press, London, 1956).
[16]B. M. Askerov, *Electron Transport Phenomena in Semiconductors* (World Scientific, Singapore, 1994).
[17]M. Ahrens, R. Merkle, B. Rahmati, and J. Maier, Phys. B: Condens. Matter **393**(1–2), 239 (2007).
[18]C. Yu, M. L. Scullin, M. Huijben, R. Ramesh, and A. Majumdar, Appl. Phys. Lett. **92**(19), 191911 (2008).